We are IntechOpen, the world's leading publisher of Open Access books Built by scientists, for scientists

4,800
Open access books available

122,000
International authors and editors

135M
Downloads

Our authors are among the

154
Countries delivered to

TOP 1%
most cited scientists

12.2%
Contributors from top 500 universities

CLARIVATE ANALYTICS BOOK CITATION INDEX INDEXED

WEB OF SCIENCE™

Selection of our books indexed in the Book Citation Index in Web of Science™ Core Collection (BKCI)

Interested in publishing with us?
Contact book.department@intechopen.com

Numbers displayed above are based on latest data collected.
For more information visit www.intechopen.com

Chapter 12

In Vitro Evaluation of Laser-Induced Periodic Surface Structures on New Zirconia/Tantalum Biocermet for Hard-Tissue Replacement

Alberto Jorge-Mora, Naroa Imaz, Nekane Frutos, Ana Alonso, Carlota García Santiago, Rodolfo Gómez-Vaamonde, Jesús Pino-Minguez, Jose Bartolomé, Gerard O'connor and Daniel Nieto

Additional information is available at the end of the chapter

http://dx.doi.org/10.5772/intechopen.70820

Abstract

This study investigates the biological response of zirconia/tantalum biocermet materials with laser-induced periodic surface structures (LIPSS) generated using a femtosecond laser working at 1030 nm wavelength. LIPSS were formed by laser radiation slightly above the applied threshold fluence. LIPSS features were characterized using techniques such as atomic force microscopy (AFM) and X-ray photoelectron spectroscopy (XPS). LIPSS were generated in this study by applying femtosecond pulses with 500 fs pulse duration at a high-repetition rate to smooth-polished zirconia/tantalum biocermet surfaces, with an original roughness value of 3.8 ± 0.2 and 3.1 ± 0.2 nm, respectively. We have demonstrated in vitro that LIPSS are an efficient option to increase osteoblastic differentiation of human bone marrow mesenchymal stem cells (hBMSCs) in ZrO_2:Ta biocermets. LIPSS created increase cell metabolism statistically (best values in 3-(4,5-dimethylthiazol-2-yl)-2,5-diphenyltetrazolium bromide (MTT) assay) and decrease inflammatory response to the material (IL-6 and TNF-alpha values). Extracellular matrix production (ECM) is produced in more quantity and cells differentiate to osteoblast easily. These differences are seen from the beginning until the endpoint (day 20).

Keywords: laser-induced periodic surface structures, LIPSS, hard-tissue replacement, zirconia/tantalum biocermet

1. Introduction

Orthopaedic surgery has experienced a big development, thanks to the evolution of the materials used, which made it possible to perform procedures, such as total hip replacement with feasibility. These procedures are common in most orthopaedic departments and the survival of these implants is critical to prevent loosening and the need for revision arthroplasty with a cost of more than 15,000 euros in total hip or knee replacement. The ideal surface to interact with bone has not been created. We can find promising results in some materials, for example, hydroxyapatite plasma coating creates early and strong integration, but it seems that this treatment experiments long-term reviews due to the loosening of the coat [1]. Multiple techniques have been proposed to increase osteointegration in metals. Probably the most accepted and used are the creation of a plasma coating with hydroxyapatite in some situations and the texturization of the metal in the microscale [2–6].

Laser processing has gained significant importance in the medical industry and is an integral part of manufacturing, for example, welding endoscopes, drilling holes in hypodermic needles and verification laser marking [2, 3]. Lasers offer high precision and repeatability, high speed and quality, accuracy, cost efficiency, minimal thermal input and noncontact [7–10]. In particular, femtosecond lasers are ideal for surface structuring because they have a minimal heat affected zone, there is rapid heating and cooling and no laser plasma interaction [11–16]. Femtosecond laser-induced periodic surface structures (LIPSS), known as "ripples," have been fabricated on material surfaces such as metals [17], polymers [18], glass, dielectric and semiconductors [19, 20]. There are a number of applications of LIPSS such as increasing the surface area and surface energy, altering the hydrophilic or hydrophobic performance of a materials' surface, improving coating adhesion, optics and tribology [21, 22]. These characteristics are of great interest for biomedical applications, in particular for hard-tissue replacement [23–25].

This study investigates the bioresponse of zirconia/tantalum biocermets (ZrO_2:Ta) with laser-induced periodic surface structures (LIPSS) produced by femtosecond laser pulses. Experiments were carried out using a Yb:KYW chirped-pulse-regenerative amplification laser system (Amplitude Systemes S-pulse HP) that delivered laser pulses with a duration of approximately 500 fs at wavelength of 1030 nm. We investigate the physical and biological response of LIPSS created using a femtosecond laser on an alloy surface. This includes determining the role of incubation and nanostructures, the physical characterization of LIPSS and the biological response of LIPSS. ZrO_2:Ta surfaces were exposed to multiple incident laser shots in air at a repetition rate of 100 kHz at various pulse energies ranging from 2 to 6 mJ. Periodic surface nanostructures were formed by exposure to laser radiation slightly above the applied threshold fluence and observed using techniques such as atomic force microscopy (AFM) and scanning electron microscopy (SEM). Section 2 introduces materials and methods. In Section 3, we describe the LIPPS fabrication procedure and results. Section 4 is devoted to biological results and Section 5 to conclusions.

http://dx.doi.org/10.5772/intechopen.70820

2. Materials and methods

2.1. Material

We have previously described the manufacturing process of the composite, were ceramic and metal powders are mixed to create the composite [21]. The samples used in this work are discs of 20 mm diameter and 2 mm thickness were cut and machined from cylindrical bars (5 mm length and 2 mm diameter).

2.2. Microstructure and surface characterization

The microstructure of samples was measured on surfaces polished down to 1 mm using a scanning electron microscopy (SEM, Phenom G2). Roughness measurements were performed by using SEM and 3D roughness reconstruction application (Phenom TM Pro Suite). The average surface roughness (Ra) was determined by measuring the surface roughness at 10 different locations over 3 samples of each type.

Morphological observation of the surfaces was undertaken by means of a Carl Zeiss Ultra Plus field emission scanning electron microscope (FE-SEM). The composition was analysed by an Oxford instruments INCA X-sight X-ray electron probe microanalyzer (EDX).The wettability of the studied materials was assessed by measuring the contact angle of deionized water drops deposited onto their surface using a KSV Instruments Cam 200 device.

Laser-induced periodic surface structures are fabricated using a fluence above the damage threshold fluence for the zirconia/tantalum biocermet. Chemical modification was analyzed using a scanning electron microscope (Hitachi S2600N). The topography was measured using an atomic force microscope (Agilent 5500).

During the fabrication process, we used an optical Nikon MM-400 microscope to visually inspect the samples; surface roughness and topography was measured using a SENSOFAR 2300 Plμ confocal microscope. Biological observations were performed using a Zeiss Microscope (Zeiss AxioVert A.1) and Zen software.

2.3. Laser processing

ZrO_2-Ta surfaces were exposed to multiple incident laser shots in air at a repetition rate of 100 kHz at various pulse energies ranging from 2 to 6 mJ. LIPSS were fabricated using a Yb:KYW laser system (Amplitude Systemes S-pulse HP) with a pulse duration of approximately 500 fs and a wavelength of 1030 nm. The beam delivery process for fabricating the LIPSS can be described as follows: the beam is focused on the top of the zirconia/tantalum biocermet surfaces using a flat-field lens (focal length = 100 mm). This kind of lens ensures a homogeneous light distribution in an area of 8×8 cm^2. The beam spot size (21 μm) was determined at $1/e^2$ of the Gaussian profile. The spatial profile of the laser was Gaussian in nature with a nominal M2 value of <1.2. The laser set-up for texturing ZrO_2-Ta surfaces with LIPSS is shown in **Figure 1**.

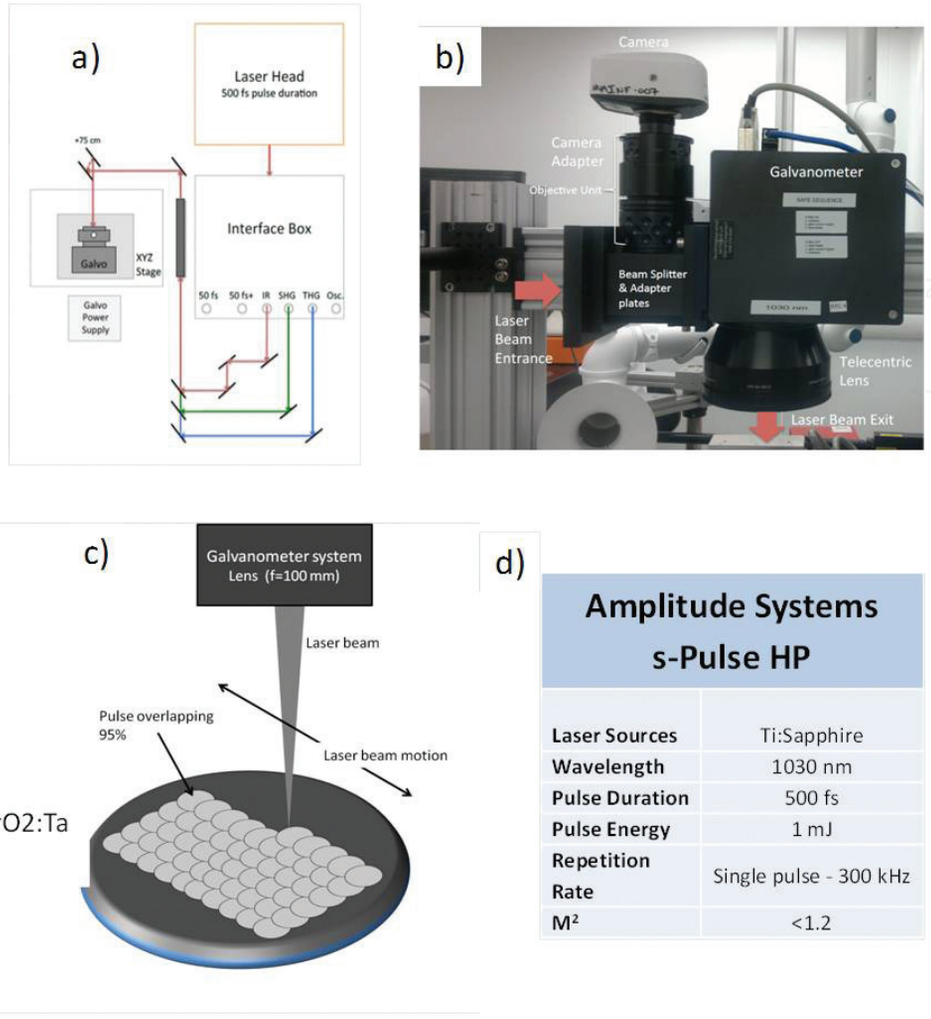

Figure 1. (a) Laser set-up and (b) beam delivery system for generating the LIPSS; (c) schematic of LIPSS fabrication process and (d) femtosecond laser characteristics.

2.4. Biological assay

We created 50 discs of the cermet. Each disc had a diameter of 6.75 mm (± 0.02 mm) and a thickness of 1.25 mm (± 0.02 mm). Once all the discs have been obtained, we proceed to polish those discs to prepare and to apply further treatments. We maintained 25 unaltered discs as a control group. In the remaining 25, we apply a laser treatment, which is explained later in detail, to create regular structures or roughness in the metallic structures of the cermet at disc surfaces. The samples used were treated with an ultrasonic bath for effective cleaning and then autoclaved (Selecta Autotester) at 121°C for 30 min. We used one disc from each group to culture mesenchymal stem cells (MSC) for 48 h to compare under direct vision cell behaviour.

After Institutional Review Board approval, and after giving consent, we obtained mesenchymal stem cells (MSC) from iliac crest of patients who were operated elective, with no previous disease and with an age between 18 and 50 years old. Under spinal anaesthesia, during the main orthopaedic procedure, we performed a puncture with a trocar in the iliac crest to aspirate bone marrow mesenchymal stem cells. We used a low-pressure technique with heparin and saline to prevent haemolysis and the formation of clots.

Afterwards, we used a Ficoll-Histopaque (Sigma-Aldrich) gradient to isolate MSC. Then, we cultured the MSC to expand them under sterile conditions until we had obtained a concentration of 25,000 cells/cm^2 as previously reported. We confirmed the desired cell concentration with a Neubauer chamber.

The survival and proliferation of hBMSCs on discs were examined with a MTT assay after 5, 10, 15 and 20 days of culture (groups of 6 discs). The MTT assays were carried out as per manufacturer's protocol (Sigma-Aldrich). Briefly, hBMSCs were seeded on the sample discs (both surfaces were tested at the same time to diminish variability) at a density of 25×10^3 cells per well in a 24-well plate. The medium was removed periodically at each time point, MTT solution was added and cells were incubated overnight. Next step was to remove the MTT solution and dissolve the purple formazan crystals in 100 mL of dimethyl sulphoxide (DMSO) by shaking the plate for 15 min (50 mL solution of each well was added into a new 24-well plate). An automated plate reader (PerkinElmer) was used to quantify the OD value by measuring the absorption at 570 nm.

Afterwards, we proceed to clean the discs to use them for remaining biological assays. We proceed to clean all surfaces chemically (to destroy all biological tissues without modifying the surface) and treated them with an ultrasonic bath for effective cleaning and then autoclaved (Selecta Autotester) at 121°C for 30 min.

To assess the amount of inflammatory cytokine concentration, both IL-6 and TNF-alpha ELISA kits (eBioscience) were performed according to the manufacturer's indications. Kits were read on a spectrophotometer at the wavelength indicated by the manufacturer.

Formation of an ECM implies the deposition of collagen (the main protein of the ECM) on the biomaterial surface. Collagen concentration was assessed by means of a total protein assay (Pierce Labs USA).

Alkaline phosphatase (ALP) protein was assessed every 5 days. Samples were lysed using Cell Lysis Buffer (Cell Signalling), collected, and spun down at 14,000× *g* for 10 min at 4°C. The supernatant was then collected to measure ALP protein levels via LabAssay ALP (Wako); protein levels were normalized by measuring total protein content via a BCA Protein Assay kit (Thermo Fisher Scientific).

Osteocalcin and osteopontin levels were assessed to gain an insight of the mesenchymal cell fate determination. Increased values of osteocalcin and osteopontin are associated with osteoblastic differentiation. Supernatants were collected at different time points and measured by ELISA kits (Thermo Fisher).

We performed a Kolmogorov-Smirnov test to confirm that values have a normal distribution. After we used a T-student test to compare rough and smooth surfaces, we accepted a p value lower than 0.05 as statistically significant.

3. Experimental results

The laser set-up for fabricating the laser-induced periodic surface structures (LIPSS) on ZrO_2: Ta surfaces consists of a Yb:KYW chirped-pulse-regenerative amplification laser system

(Amplitude Systemes S-pulse HP). The laser set-up used for fabricating the LIPSS is described in Section 2.3. **Figure 1** shows the laser set-up for fabricating the LIPSS on ZrO_2:Ta samples.

The laser system for fully texturing materials with LIPSS is shown in **Figure 1c**. For fabricating the LIPSS, the incident direction of the laser was orthogonal to the sample plane. Each sample was fully textured by combining an aligned array of spots at a laser wavelength of 1030 nm. The irradiation conditions for both materials were applied fluence of 0.30 J/cm^2, laser spot of 21 μm, wavelength of 1030 nm, repetition rate of 100 kHz, pulse width of 500 fs and sample scan speed of 200 mm/s; the sample was fully textured using highly over-lapped (95%) pulses. This method is very effective in accelerating the processing times while the obtained results are similar to conventional pulsed-laser treatments for creating LIPSS. Fluence was calculated using Eqs. (2) and (3). The applied threshold fluence for one pulse was previously calculated and it was found that with increasing number of laser pulses, the threshold fluence decreases [26].

The calculations for determining applied threshold fluence (ϕ_{th}) and (ϕ_0) are obtained according to the method of Liu et al. [27]. The spatial fluence, (ϕ_r), for a Gaussian beam is given by:

$$\phi(r) = \phi_0 e^{-2r^2/\omega_0^2} \tag{1}$$

where ϕ_0 is the peak fluence in the beam, r is the distance from the centre of the beam and ω_0 is the Gaussian spot radius (1/e^2). The maximum fluence and the pulse energy, E_p, are related by:

$$\phi_0 = \frac{2E_p}{\pi\omega_0^2} \tag{2}$$

The peak fluence is related to the diameter of the ablated spot

$$D^2 = 2\omega_0^2 \ln\left(\frac{\phi_0}{\phi_{th}}\right) \tag{3}$$

where D^2 is the maximum diameter of the damaged region zone. It is possible to determine the beam radius using the value for ω_0 from the plot of D^2 versus the logarithm of the pulse energy. Once ω_0 is calculated, fluence values can then be found using Eq. (3). By plotting D^2 versus the natural log of the applied laser fluence and extrapolating the D^2 line to zero, ϕ_{th} can be calculated.

Figure 2 shows a polished ZrO_2:Ta sample used for generating ripples that exhibits a roughness average of 3.7 ± 0.2 nm.

LIPPS were fabricated on ZrO_2:Ta samples illustrated on **Figure 2** by irradiation with a p-polarized femtosecond laser. The laser parameters used for generating the LIPSS were repetition rate of 100 kHz, pulse width of 500 fs, sample scan speed of 200 mm/s and 50 passes of highly over-lapped (95%). In **Figure 3**, we can see the typical fabricated LIPSS or ripples observed in the scanning electron microscopy images. Periodical micropatterns were generated in ZrO_2:Ta using the abovementioned laser parameters at 200 mw laser power.

As shown in **Figure 3**, periodic structures were generated on tantalum while zirconia shows irregular structures at surface. The period of the surface ripples is significantly smaller than the

http://dx.doi.org/10.5772/intechopen.70820

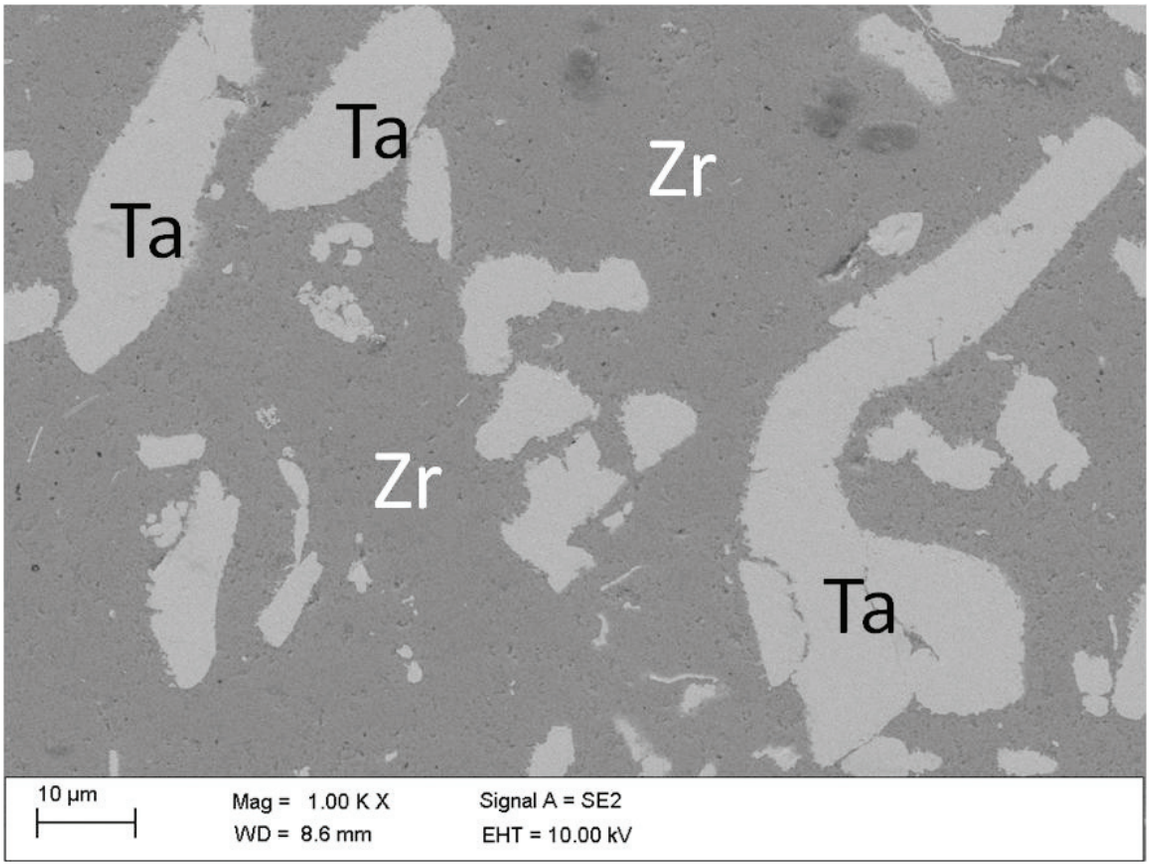

Figure 2. FE-SEM image of the ZrO_2:Ta cermet used for performing experiments.

wavelength of the incident laser beam. The period of ripples is estimated to be 760 ± 48 nm and the depth is 251 ± 7 nm when exposed to a 1030 nm, and the roughness average is 54 ± 2 nm. The depth of LIPSS depends on various parameters such as absorption coefficient, thermal diffusion and radiative cooling of the material. The effective penetration depth ($\alpha-1$) is proportional to the laser wavelength. After femtosecond laser exposure, the alloy changes its optical penetration depth, as the material become amorphous. After multiple-pulse exposure which incorporates rapid heating and cooling cycles, the zirconia/tantalum material could evolve toward a metallic-like glass which would favor deeper surface structures [28].

Wettability results assessed in aqueous medium are presented in **Figure 4**. Since liquid ZrO_2:Ta interfacial tension is not easy to measure directly, the contact angle of a deionized water droplet on the studied cermets was used to indicate surface wettability. The equilibrium contact angle (θeq) of a liquid drop on an ideal solid surface is defined by Young's equation [29]:

$$\sigma\text{LV}\cos\theta\text{eq} = \sigma SV - \sigma SL \tag{4}$$

where σSV, σSL and σLV are the interfacial tensions between solid-gas, solid-liquid and liquid-gas phases, respectively. Our results indicate that the as-cast cermet shows high wettability with a contact angle value of 81.2°. On the other hand, laser-treated ZrO_2:Ta alloy presents significantly higher contact angle (113.5°), that is, it shows a more hydrophobic character.

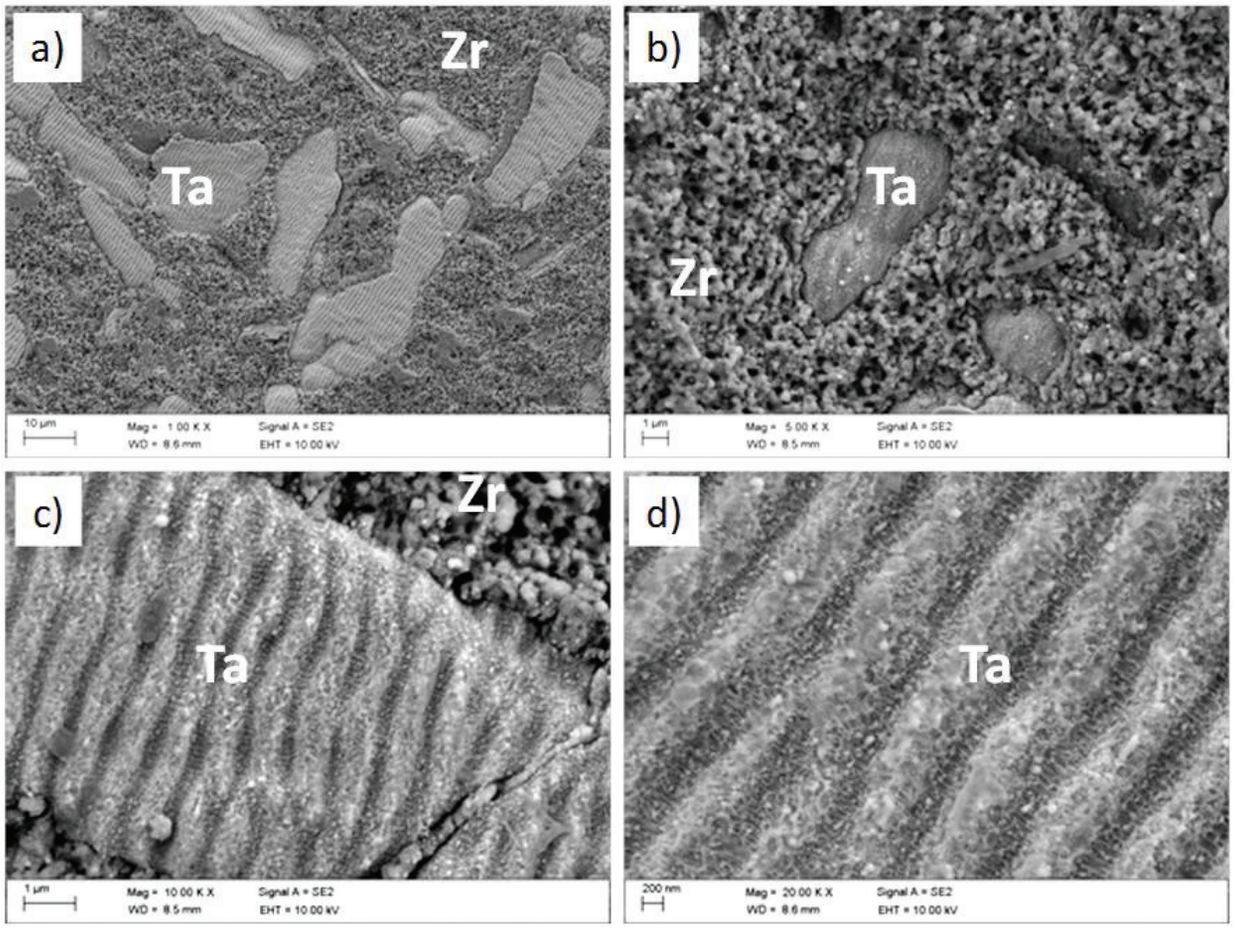

Figure 3. FE-SEM images of the fabricated micropatterned structures on ZrO_2:Ta (Ta: Tantalum; Zr: Zirconia) at different magnifications.

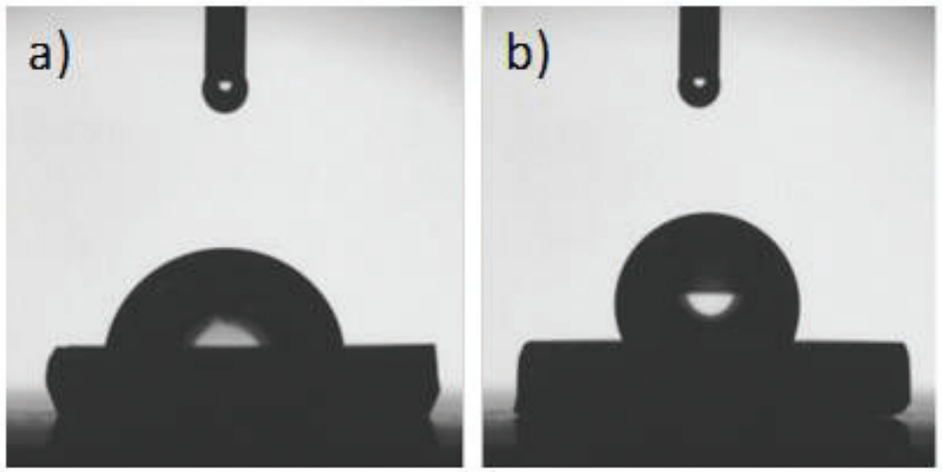

Figure 4. Photographs of as-deposited water droplets onto the surface of (a) as-cast and (b) ZrO_2-Ta with ripples.

Considering γlv constant for a certain liquid in a particular environment, the observed variability in wettability values could be ascribed to variations in γsv and γsl, caused by the hierarchical structures fabricated on ZrO_2:Ta surface by the applied laser process. LIPSS

nanopattern may be responsible for the observed hydrophobicity increase, which could also be influenced by the intrinsic change in the surface chemistry with the exposure to air after the laser fabrication process [30].

Cell adhesion and several cellular functions are strongly influenced by the surface properties of a material. It has been proved that surface chemistry, energy, topography and wettability are key factors that affect protein adsorption and blood coagulation, which may have an impact on the adhesion, migration and differentiation of osteogenic cells, playing an important role in implants' osteointegration [31, 32]. In the studied cases, an increase in the protein adsorption and osteoblast differentiation parameters for laser-treated surfaces was observed, in spite of their lower wetting properties. The higher specific surface area offered by the fabricated nanostructures can play a decisive role in providing more adsorption sites for bioactive molecules and proteins, mitigating the effect of surface hydrophobicity [33].

4. Biological results

On the biological side, one of the main challenges in this study was to investigate the cells' behaviour when cultured over nanometric structures (LIPPS) to increase osteoblastic differentiation. After fabricating laser-induced periodic surface structures, we studied the behaviour of

		SMOOTH 5	LIPSS 5	SMOOTH 10	LIPSS 10	SMOOTH 15	LIPSS 15	SMOOTH 20	LIPSS 20
MTT	Mean	0.711	0.722	0.784	0.767	0.868	0.917	0.943	0.980
	Std. deviation	0.046	0.053	0.067	0.051	0.061	0.119	0.079	0.085
IL-6	Mean	0.018	0.019	0.026	0.023	0.031	0.031	0.032	0.030
	Std. deviation	0.002	0.002	0.004	0.003	0.003	0.003	0.002	0.003
TNF-alpha	Mean	0.018	0.018	0.023	0.023	0.024	0.024	0.045	0.044
	Std. deviation	0.001	0.002	0.003	0.002	0.002	0.002	0.003	0.007
ECM	Mean	0.033	0.029	0.044	0.055	0.325	0.452	0.333	0.425
	Std. deviation	0.026	0.015	0.028	0.031	0.044	0.034	0.040	0.052
AF	Mean	0.544	1.037	0.580	1.123	0.626	1.224	0.679	1.317
	Std. deviation	0.038	0.198	0.026	0.145	0.047	0.073	0.033	0.132
OSC	Mean	0.539	0.639	0.575	0.624	0.622	0.778	0.601	0.787
	Std. deviation	0.052	0.043	0.049	0.069	0.063	0.069	0.049	0.050
OSP	Mean	0.716	0.838	0.765	0.825	0.837	0.831	0.922	0.884
	Std. deviation	0.057	0.075	0.077	0.050	0.130	0.123	0.059	0.076

Table 1. Mean value for each assay and time point with the standard deviation.

bone marrow mesenchymal stem cells compared to polished surfaces. We cultured hBMSCs in a concentration of 25,000 cells/cm^2 in the surfaces created for 20 days. We determined MTT, TNF-alpha, IL-6, collagen production, alkaline phosphatase, osteopontin and osteocalcin for every 5 days until day 20. **Table 1** summarizes the average of all measurements for each assay.

MTT values in both surface treatments were similar (**Figure 5**), without reaching the statistical significance at any time point of control. Inflammatory response of both materials described by IL-6 and TNF-alpha values was also similar, with no difference between surfaces. We found very low values for both surfaces. **Figure 5** shows the data obtained for MTT assay with the standard deviation.

We found a significant difference in ECM production (**Figure 6**) and osteoblast differentiation parameters (FA, OSC and OSP). ECM production was statistically increased in LIPSS surfaces at days 15 and 20. Alkaline phosphatase activity was increased at all time point controls. Osteocalcin levels were also elevated at every control, but at day 10 there was no statistical difference. Osteopontin values were also superior to control in every control, but only reached statistical difference at day 5. **Figure 6** shows the data obtained for ECM assay with the standard deviation.

Confocal microscopic image (**Figure 7**) showed a polarization of cells in the metal area (where LIPSS are generated). In the surface where the ceramic is present, we can see a disordered pattern seen in most of the smooth surfaces.

We can see a transition between LIPSS and the ceramic surface. In the upper left corner, we can see a polarization of the long axis of the cell, which is not seen in the ceramic surface

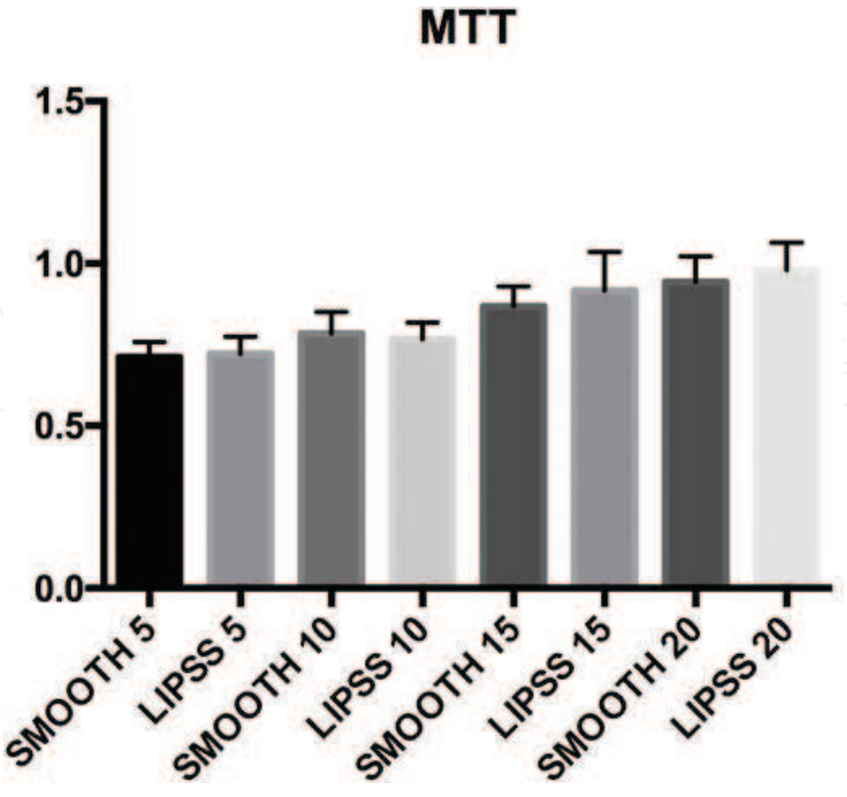

Figure 5. Data obtained for MTT assay with the standard deviation.

http://dx.doi.org/10.5772/intechopen.70820

(lower right corner). **Figure 8** shows the images obtained on smooth surfaces, which showed a nonorganized mess of cells without polarization.

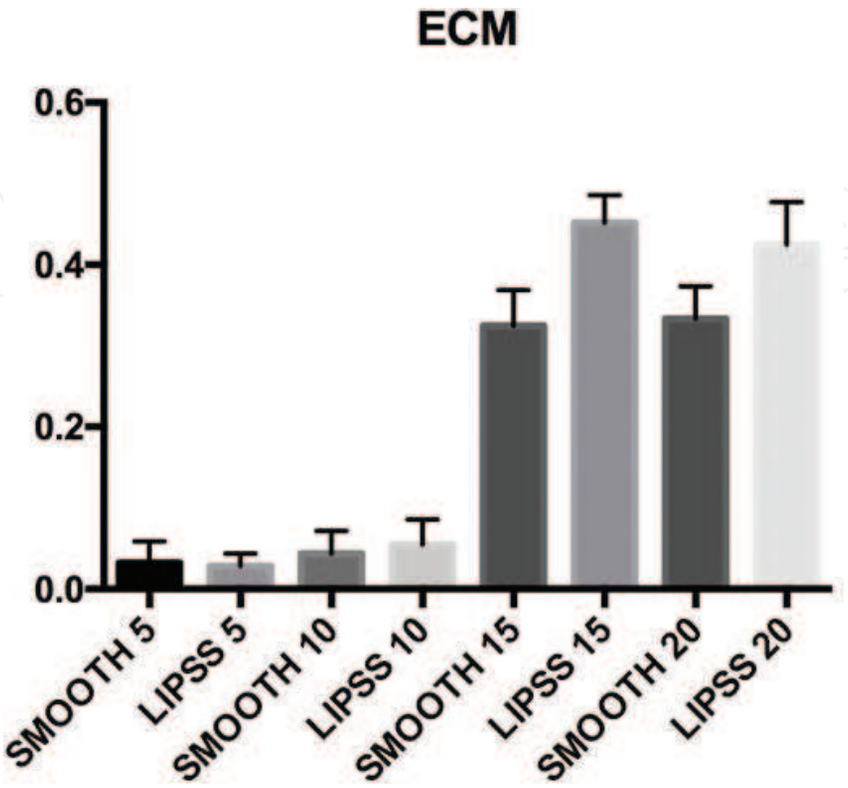

Figure 6. Data obtained for ECM assay with the standard deviation.

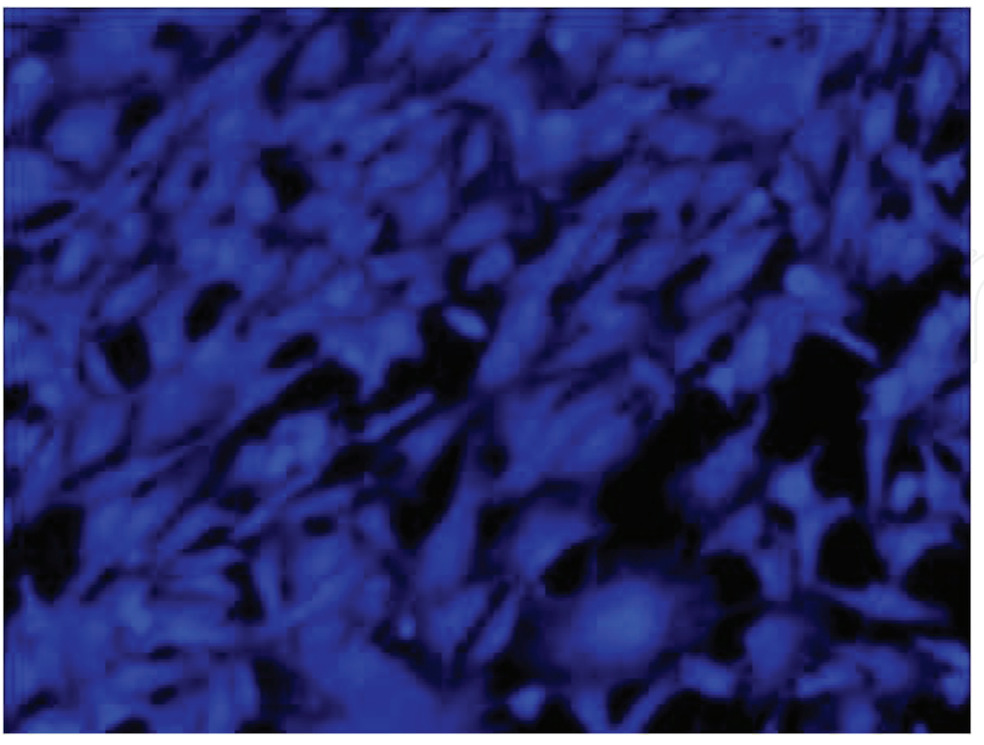

Figure 7. Confocal image of a treated surface.

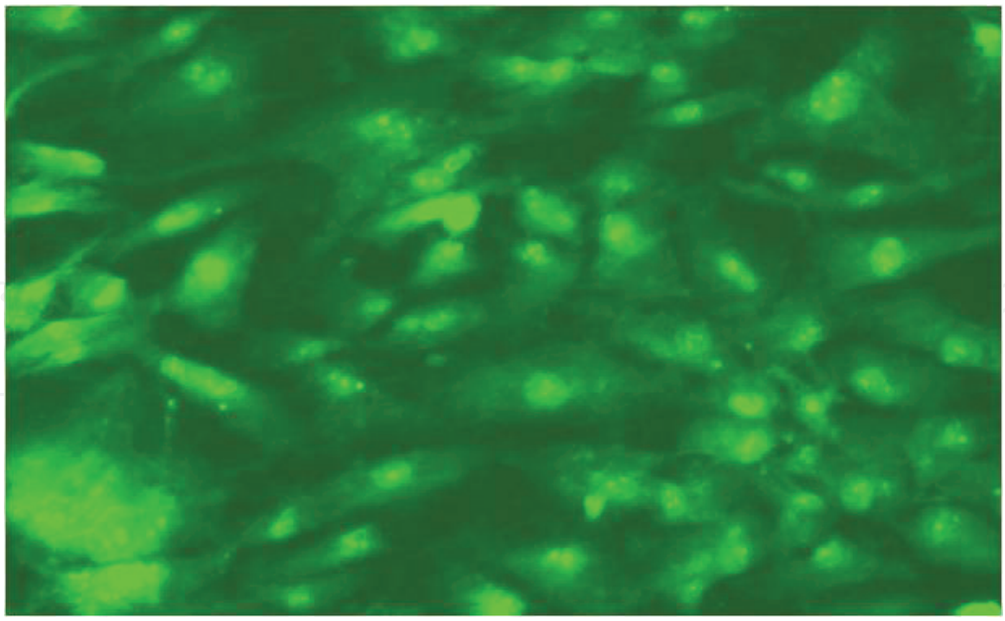

Figure 8. Confocal image of the smooth surface.

5. Conclusions

We have demonstrated in vitro that LIPSS are an efficient option to increase osteoblastic differentiation of hBMSCs in ZrO_2:Ta biocermets. When we create a laser-induced periodic surface with a femtosecond laser, we found that proliferation and inflammatory response are not increased when compared to a smooth surface. We know that LIPSS in metals decreases hydrophobicity compared to smooth surfaces, but in cermet this situation is not seen. We believe that we found a dual phenomenon. In the metal area of the cermet, the contact angle is decreased, but in the ceramic area, the transformation phase seen with this laser treatment increases the contact angle and the hydrophobicity. The optimization of the laser treatment probably will improve the wettability minimizing the transformation phase.

We can see an increase in the ECM in treated surfaces at days 15 and 20. These values add more significance to the values obtained for osteoblastic differentiation.

With values of proliferation similar in both materials, we found an increase in osteoblastic differentiation in LIPSS created over ZrO_2:Ta compared to smooth surfaces. This increase is demonstrated by higher values in the studied assays of alkaline phosphatase, osteocalcin and osteopontin production at every control point. This behaviour is seen in metals such as titanium and tantalum. This situation is similar to previous studies that demonstrate a more biological activity in LIPSS surfaces compared to smooth ones.

We can conclude that creating laser-induced periodic surfaces is a promising and cheap modification to increase osteoblastic response to a material, without adding chemicals or new materials. Optimization of the laser fluence and parameters will increase this effect, minimizing the transformation phenomenon in the ceramic area, but creating LIPSS in the metal islands.

Acknowledgements

D. Nieto is grateful to the Consellería de Cultura, Spain for the support under the Galician Program for Research Innovation and Growth (2011–2015) (I2C Plan).

Author details

Alberto Jorge-Mora[1,2], Naroa Imaz[3], Nekane Frutos[3], Ana Alonso[2], Carlota García Santiago[4], Rodolfo Gómez-Vaamonde[1,2], Jesús Pino-Minguez[1,5], Jose Bartolomé[6], Gerard O'connor[6] and Daniel Nieto[7,8]*

*Address all correspondence to: daniel.nieto@usc.es

1 SERGAS (Galician Health Service), Universidad de Santiago de Compostela, Santiago de Compostela, Spain

2 IDIS (Musculoskeletal Pathology Group), Santiago de Compostela, Spain

3 Surface Engineering Division, IK4-CIDETEC, San Sebastián, Spain

4 Department of Pharmacology, Universidade de Santiago de Compostela, Spain

5 IDIS (NEIRID Group), Orthopaedic Department, Santiago de Compostela, Spain

6 Instituto de Ciencia de Materiales de Madrid (ICMM), Consejo Superior de Investigaciones Científicas (CSIC), Madrid, Spain

7 NCLA / Inspire Labs, School of Physics, National University of Ireland, Galway, Ireland

8 Photonics4Life Research Group, Departamento de Física Aplicada, Facultad de Física, Universidade de Santiago de Compostela, Santiago de Compostela, Spain

References

[1] Arifin A, Sulong AB, Muhamad N, Syarif J, Ramli MI. Material processing of hydroxyapatite and titanium alloy (HA/Ti) composite as implant materials using powder metallurgy: A review. Materials and Design. 2014;**55**:165-175

[2] Coathup MJ, Blunn GW, Mirhosseini N, Erskine K, Liu Z, Garrod DR, et al. Controlled laser texturing of titanium results in reliable osteointegration. Journal of Orthopaedic Research. 2016

[3] Kurella A, Dahotre NB. Review paper: Surface modification for bioimplants: The role of laser surface engineering. Journal of Biomaterials Applications. 2005;**20**(1):5-50

[4] Rokkum M, Reigstad A, Johansson CB. HA particles can be released from well-fixed HA-coated stems: histopathology of biopsies from 20 hips 2–8 years after implantation. Acta Orthopaedica Scandinavica. 2002;**73**(3):298-306

[5] Han CD, Shin KY, Lee HH, Park KK, Yang IH, Lee WS. The results of long-term follow-up of total hip arthroplasty using hydroxyapatite-coated cups. Hip & Pelvis. 2015;**27**(4):209-215

[6] Martinez-Calderon M, Manso-Silvan M, Rodriguez A, Gomez-Aranzadi M, Garcia-Ruiz JP, Olaizola SM, et al. Surface micro- and nano-texturing of stainless steel by femtosecond laser for the control of cell migration. Scientific Reports. 2016;**6**:36296

[7] Nieto D, Delgado T, Flores-Arias MT. Fabrication of microchannels on soda-lime glass substrates with a Nd:YVO_4 laser. Optics and Lasers in Engineering. 2014;**63**:11-18

[8] Nieto D, Couceiro R, Aymerich M, Lopez-Lopez R, Abal M, Flores-Arias MT. A laser-based technology for fabricating a soda-lime glass based microfluidic device for circulating tumour cell capture. Colloids and Surfaces B: Biointerfaces. 2015;**134**:363-369

[9] Chen M-F, Chen Y-P, Hsiao W-T, Gu Z-P. Laser direct write patterning technique of indium tin oxide film. Thin Solid Films. 2007;**515**:8515-8518

[10] Nieto D, McGlynn P, de la Fuente M, Lopez-Lopez R, O'connor GM Laser microfabrication of a microheater chip for cell culture outside a cell incubator Colloids Surf B Biointerfaces. 2017;**154**:263-269

[11] Mannion PT, Magee J, Coyne E, O'Connor GM, Glynn TJ. The effect of damage accumulation behaviour on ablation thresholds and damage morphology in ultrafast laser micromachining of common metals in air. Applied Surface Science. 2004;**233**:275-287

[12] Hwang TY, Vorobyev AY, Guo CL. Ultrafast dynamics of femtosecond laser-induced nanostructure formation on metals. Applied Physics Letters. 2009;**95**

[13] Hwang TY, Guo CL. Femtosecond laser-induced blazed periodic grooves on metals. Optics Letters. 2011;**36**:2575-2577

[14] Bonse J, Kruger J, Hohm S, Rosenfeld A. Femtosecond laser-induced periodic surface structures. Journal of Laser Applications. 2012;**24**

[15] Gurevich EL, Gurevich SV. Laser induced periodic surface structures induced by surface plasmons coupled via roughness. Applied Surface Science. 2014;**302**:118-123

[16] Sedao X, Maurice C, Garrelie F, Colombier JP, Reynaud S, Quey R, Blanc G, Pigeon F. Electron backscatter diffraction characterization of laser-induced periodic surface structures on nickel surface. Applied Surface Science. 2014;**302**:114-117

[17] Huynh TTD, Petit A, Semmar N. Picosecond laser induced periodic surface structure on copper thin films. Applied Surface Science. 2014;**302**:109-113

[18] Perez S, Rebollar E, Oujja M, Martin M, Castillejo M. Laser-induced periodic surface structuring of biopolymers. Applied Physics A: Materials Science & Processing. 2013; **110**:683-690

[19] Kumar B, Soni RK. Pulsed-laser-induced photochemical growth of the periodic surface structure on InP. Semiconductor Science and Technology. 2009;**24**

[20] Hohm S, Herzlieb M, Rosenfeld A, Kruger J, Bonse J. Formation of laserinduced periodic surface structures on fused silica upon two-color double-pulseirradiation. Applied Physics Letters. 2013;**103**

[21] Bartolome JF, Moya JS, Couceiro R, Gutierrez-Gonzalez CF, Guiti F, Martinez-Insua A. In vitro and in vivo evaluation of a new zirconia/niobium biocermet for hard tissue replacement. Biomaterials. 2016;**76**:313-320

[22] Daminelli G, Krüger J, Kautek W. Femtosecond laser interaction with silicon under water confinement. Thin Solid Films. 2004;**467**:334-341

[23] Suchanek W, Yoshimura M. Processing and properties of hydroxyapatite-based biomaterials for use as hard tissue replacement implants. Journal of Materials Research. 1998;**13**:94-117

[24] Karageorgiou V, Kaplan D. Porosity of 3D biomaterial scaffolds and osteogenesis. Biomaterials. 2005;**26**:5474-5491

[25] Vasconcellos LMRd, Oliveira MVd, Graça MLdA, Vasconcellos LGOd, Carvalho YR, Cairo CAA. Porous titanium scaffolds produced by powder metallurgy for biomedical applications. Materials Research. 2008;**11**:275-280

[26] Nieto D, Arines J, O'connor GM, flores-Arias MT. Single-pulse laser ablation threshold of borosilicate, fused silica, sapphire, and soda-lime glass for pulse widths of 500 fs, 10 ps, 20 ns. Applied Optics. 2015;**54**(29):8596-8601

[27] Liu X-L, Cheng W, Petrarca M, Polynkin P. Measurements of fluence profiles in femtosecond laser filaments in air. Optics Letters. 2016;**41**(20):4751-4754

[28] McDaniel C, Gladkovskaya O, Flanagan A, Rochev Y, O'Connor GM. In vitro study onthe response of RAW264.7 and MS-5 fibroblast cells on laser-induced periodic surfacestructures for stainless steel alloys. RSC Advances. 2015;**5**:42548-42558

[29] Young T. Philosophical Transactions of the Royal Society of London. 1805;**95**:65

[30] Martínez-Calderón M, Rodríguez A, Dias A, Morant-Miñana MC, Gómez-Aranzadi M, Olaizola SM. Femtosecond laser fabrication of highly hydrophobic stainless steel surface with hierarchical structures fabricated by combining ordered microstructures and LIPSS. Applied Surface Science. 2015;**374**:81-89

[31] Wennerberg A, Jimbo R, Stübinger S, Obrecht M, Dard M, Berner S. Nanostructures and hydrophilicity influence osseointegration – A biomechanical study in the rabbit tibia. Clinical Oral Implants Research. 2014;**25**:1041

[32] Kenar H, Akman E, Kacar E, Demir A, Park H, Abdul-Khaliq H, AktaCs KE. Femtosecond laser treatment of 316L improves its surface nanoroughness and carbon content and promotes osseointegration: An in vitro evaluation. Colloids and Surfaces B. 2013;**108**:305-312

[33] Kopf BS, Ruch S, Berner S, Spencer ND, Maniura-Weber K. The role of nanostructures and hydrophilicity in osseointegration: In-vitro protein-adsorption and blood-interaction studies. Journal of Biomedical Materials Research Part A. 2015;**2015**(103A):2661-2672

IntechOpen